Available online at www.sciencedirect.com
SCIENCE DIRECT®
Nuclear Physics A 728 (2003) 275–284
NUCLEAR PHYSICS A
www.elsevier.com/locate/npe

Determination of $^{11}C(p,\gamma)^{12}N$ astrophysical S-factor via measurement of $^{11}C(d,n)^{12}N$ reaction

Weiping Liu *, Zhihong Li, Xixiang Bai, Bing Guo, Sheng Zeng, Yongshou Chen, Shengquan Yan, Baoxiang Wang, Gang Lian, Yun Lu, Kaisu Wu, Nengchuan Shu

China Institute of Atomic Energy, P.O. Box 275(80), Beijing 102413, PR China

Received 11 February 2003; received in revised form 4 August 2003; accepted 11 August 2003

Abstract

Angular distribution of the $^{11}C(d,n)^{12}N$ reaction at $E_{cm} = 9.8$ MeV was measured in inverse kinematics with the secondary ^{11}C beam. The experimental data were analyzed with DWBA calculations and thereby the asymptotic normalization coefficient, $(C^{^{12}N}_{p_{eff}})^2 = (C^{^{12}N}_{p_{1/2}})^2 + (C^{^{12}N}_{p_{3/2}})^2$, was extracted to be 2.86 ± 0.91 fm^{-1} for the virtual decay $^{12}N \to {}^{11}C + p$. The zero energy astrophysical S-factor for the direct capture $^{11}C(p,\gamma)^{12}N$ reaction was then derived to be 0.157 ± 0.050 keV b. We have also estimated the contributions from resonant captures into the first- and second excited states of ^{12}N and the interference between direct capture into the ground state and resonant capture into the second excited state. The temperature dependences of the direct capture, resonant capture and total reaction rates for $^{11}C(p,\gamma)^{12}N$ were derived. The present work shows that the direct capture dominates the $^{11}C(p,\gamma)^{12}N$ in the wide energy range of astrophysical interest except the ranges corresponding to two resonances.

PACS: 26.20.+f; 25.60.Je; 24.50.+g; 25.45.Hi

Keywords: NUCLEAR REACTIONS $^{2}H(^{11}C, ^{12}N)$, $E_{cm} = 9.8$ MeV; measured $\sigma(\theta)$; deduced asymptotic normalization coefficient. $^{11}C(p,\gamma)$, $E =$ low; deduced astrophysical S-factor, reaction mechanism features. DWBA analysis.

* Corresponding author.
E-mail address: wpliu@iris.ciae.ac.cn (W. Liu).

0375-9474/$ – see front matter
doi:10.1016/j.nuclphysa.2003.08.017

1. Introduction

The proton- and α-capture reactions on proton-rich unstable nuclei of $A \leqslant 13$ involved in the hot pp chains are thought to be another alternative way to the 3α process for transforming material from the pp chains to the CNO nuclei in the peculiar astrophysical sites where the temperature and density are high enough so that the capture reaction becomes faster than the competing β decay [1–3]. These linking reactions between the nuclei in the pp chains and the CNO nuclei might be of immense importance for the evolution of massive stars with very low metallicities.

One of the key reactions in the hot pp chains is the $^{11}\mathrm{C}(\mathrm{p},\gamma)^{12}\mathrm{N}$ which is believed to play an important role in the evolution of Pop III stars. As a result of the low Q-value, its cross section at astrophysically relevant energies is likely dominated by the direct capture into the 1^+ ground state of ^{12}N, and the resonant captures into the first and second excited states of ^{12}N at 2^+ 0.960 MeV and 2^- 1.191 MeV, respectively.

The $^{11}\mathrm{C}(\mathrm{p},\gamma)^{12}\mathrm{N}$ reaction has increasingly attracted the theoretical and experimental studies. However, it is very difficult to directly measure this reaction at energies of astrophysical interest because of the vanishing small cross section and low intensity of the available ^{11}C beam at present. Wiescher et al. derived the gamma widths of the 2^+ and 2^- states in ^{12}N equal to 2.59 and 2.0 meV from the life time of the first excited state in ^{12}B and the systematic rule of E1 matrix elements in light nuclei respectively, under the assumption of a 100% branching ratio to the ground state in ^{12}N [1]. Subsequently, Descouvement and Baraffe performed a microscopic cluster model calculation which gave $\Gamma_\gamma = 140$ meV for the 2^- state [2], and the repeated calculation yielded an updated value of 68 meV [3]. The Coulomb-dissociation experiment of ^{12}N by Lefebvre et al. derived $\Gamma_\gamma = 6.0^{+7}_{-3.5}$ meV for the 2^- state and an estimate of astrophysical S-factor for the direct capture [4], whereas a similar measurement by Minemura et al. yielded $\Gamma_\gamma = 13$ meV [5]. Recently, Timofeyuk and Igamov have performed a theoretical calculation of the direct capture contribution to the $^{11}\mathrm{C}(\mathrm{p},\gamma)^{12}\mathrm{N}$ reaction, derived S-factor at zero energy S(0) equal to 0.149 and $0.111^{+0.025}_{-0.020}$ keV b based on two different methods, respectively [6]. Most recently, Tang et al. have indirectly studied the direct capture reaction $^{11}\mathrm{C}(\mathrm{p},\gamma)^{12}\mathrm{N}$ by measuring the angular distribution of the $^{14}\mathrm{N}(^{11}\mathrm{C},^{12}\mathrm{N})^{13}\mathrm{C}$ peripheral transfer reaction and using the asymptotic normalization coefficient (ANC) approach [7].

The ANC approach has proved to be very effective in determining the direct capture contribution to (p,γ) or (n,γ) reaction through the measurement of one-nucleon transfer reaction [7–12]. In present work, we have measured the angular distribution of the proton transfer reaction $^{11}\mathrm{C}(\mathrm{d},\mathrm{n})^{12}\mathrm{N}$ with a 63.4 MeV secondary ^{11}C beam to extract the ANC for virtual decay $^{12}\mathrm{N} \rightarrow {}^{11}\mathrm{C} + \mathrm{p}$, and then calculated the direct capture S-factor and rate for the $^{11}\mathrm{C}(\mathrm{p},\gamma)^{12}\mathrm{N}$ reaction. The total S-factor and reaction rate including the direct capture, the resonant captures into the first and second excited states of ^{12}N as well as the interference between direct capture and resonant capture into the second excited state were also presented.

2. Experimental details and results

The experiment was carried out using the secondary beam facility [13,14] of the HI-13 tandem accelerator at China Institute of Atomic Energy, Beijing. The experimental setup and procedures are similar to the previously reported [9,15], as shown in Fig. 1. A 78.2 MeV ^{11}B primary beam from the tandem accelerator impinged on a 4.8 cm long H_2 gas cell at a pressure of 1.5 atm. The front and rear windows of the gas cell were Havar foils, each in thickness of 1.9 mg/cm^2. The ^{11}C ions were produced through the ^{1}H(^{11}B, ^{11}C)n reaction. After the magnetic separation and focus, the 63.4 MeV ^{11}C secondary beam was delivered. The typical purity of ^{11}C beam was about 70–80%. The main contaminants in the beam were ^{11}B ions out of the ^{11}B Rutherford scattering in the windows of the gas cell as well as beam tube. The ^{11}C beam was then collimated with two apertures in diameter of 3 mm and directed onto a 1.5 mg/cm^2 thick $(CD_2)_n$ target in diameter of 12 mm to study the ^{11}C(d, n)^{12}N reaction. The size of beam spot on the target was 3 mm in diameter because the target was very close to the second aperture (the separation $\leqslant$ 10 mm). The beam energy spread on the target was 1.79 MeV FWHM for long-term measurement. The beam angular divergence was about $\pm 0.3°$ after the collimation, based on the beam optics calculation. A 1.8 mg/cm^2 thick C target was used for the background measurement.

The reaction products ^{12}N were detected and identified with an energy loss (ΔE) vs. residual energy (E_r) telescope consisting of a 21.7 μm silicon ΔE detector and a 300 μm 10-annular silicon E_r detector. After a careful adjustment, the angular uncertainty resulting from the coaxiality for the centers of two collimators and 10-annular E_r detector was less than 0.01° which was calibrated with a lasing light emitter placed 4 m upstream of the target. The center hole of 10-annular E_r detector was backed by an independent 300 μm silicon detector. By the use of 10-annular E_r detector, the emerging angles of the reaction products can be directly determined from the geometrical arrangement, and thus reliable angular information can be obtained. The solid angle of telescope enabled 100%

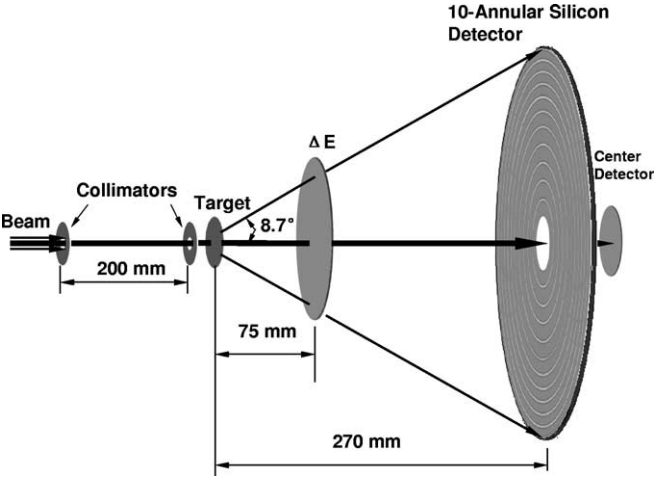

Fig. 1. Schematic experimental set-up.

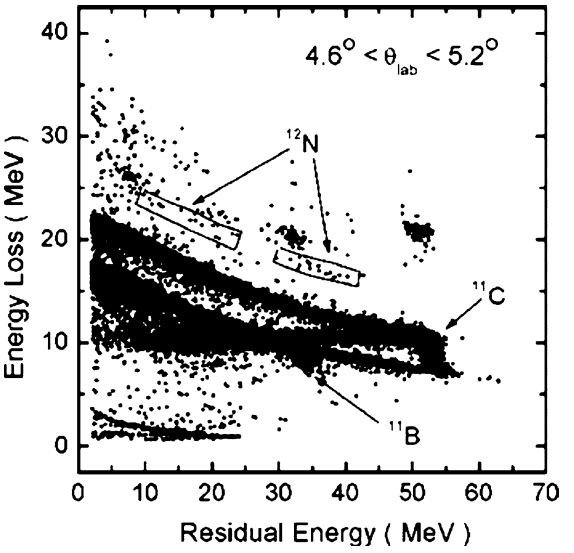

Fig. 2. Scatter plot of energy loss (ΔE) vs. residual energy (E_r) for $(CD_2)_n$ target corresponding to the 5th annulation of the 10-annular detector. The two dimension cuts for ^{12}N events were determined with Monte Carlo simulation.

detection of ^{12}N ions from the $^{2}H(^{11}C,^{12}N)n$ reaction owing to the inverse kinematics. The incident ^{11}C ions recorded by the $\Delta E - E_r$ telescope simultaneously served for the precise beam normalization. We have performed a test experiment to check the efficiency of each annulation and the dead intervals of the E_r detector by using a ^{239}Pu α source. This measurement, after normalized to the calculated solid angles, yielded an isotropic angular distribution within the statistical uncertainties, thus demonstrated the correctness of the solid angle calculation. The energy calibration of the $\Delta E - E_r$ detectors was carried out by combining the use of α source, magnetic rigidity parameter of ^{11}C beam and precision research pulser.

The measurement for the $(CD_2)_n$ target accumulated approximately 1.26×10^8 ^{11}C projectiles, while the background measurement with the carbon target about 5.0×10^7. As an example, Fig. 2 shows the 5th annulation scatter plot of ΔE vs. E_r for the $(CD_2)_n$ target. The two dimension cuts of ^{12}N events for each annulation were determined with a Monte Carlo simulation, taking the beam spot size, energy spread, angular divergence, and the target thickness into account. Fig. 3 displays the comparison of the events from $(CD_2)_n$ target with the background from carbon target for the 5th annulation, together with the energy ranges of ^{12}N events determined by Monte Carlo simulation.

After the background subtraction and the dead area correction for the center and 10-annular detectors, the resulting angular distribution in center of mass frame is given in Fig. 4 and Table 1. The differential cross section errors resulted from the statistics and the uncertainties in setting the two dimension cuts of ^{12}N events through Monte Carlo simulation. The angular uncertainties arose from five factors, which were the beam angular divergence, beam spot size, multiple scattering in target and ΔE detector, and the width of each annulation, respectively. We performed a Monte Carlo simulation to determine

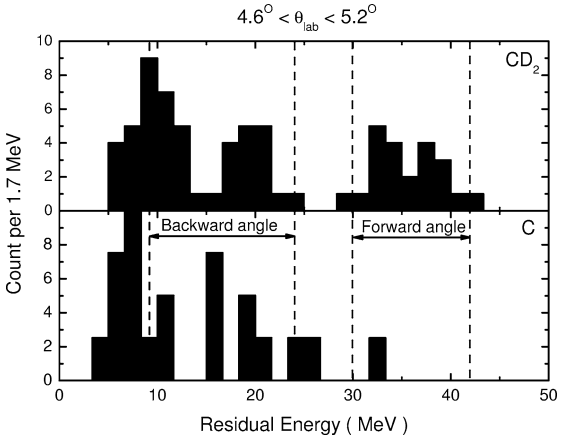

Fig. 3. Comparison of the events from $(CD_2)_n$ target with the background from carbon target for the 5th annulation. The energy ranges of ^{12}N events marked with dashed lines were obtained through Monte Carlo simulation.

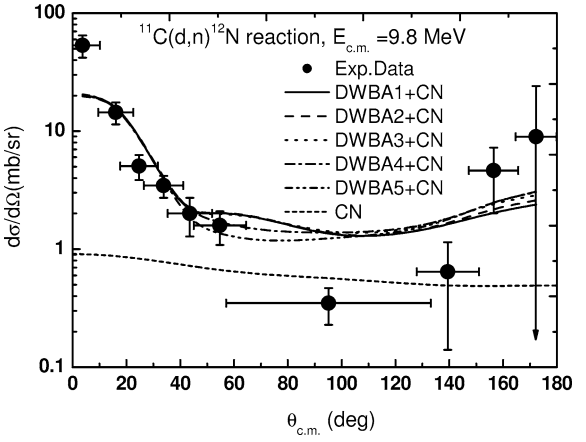

Fig. 4. Experimental angular distribution of $^{11}C(d, n)^{12}N$ reaction at $E_{cm} = 9.8$ MeV, together with DWBA calculations using 5 sets of optical potential parameters and compound nucleus calculation.

the multiple scattering in target and ΔE detector. For the 5th annulation, the above five factors were 0.30°, 0.27°, 0.16°, 0.41° and 0.28° correspondingly, and the total angular standard deviation was 0.66° in laboratory frame. The original data points in the range of $\theta_{cm} = 61$–$130°$ have merged to accord with the enlarged angular uncertainty due to inverse kinematics and finite energy resolutions. Because of the poor ratio of effect to background at back angles, the corresponding data points have also merged.

The $^{11}C(d, n)^{12}N$ reaction at present energy is dominated by the peripheral process, which was verified by changing the radial parameter limit in DWBA calculations. We have also calculated the compound nucleus (CN) contribution with the code in Ref. [16], as shown in Fig. 4. After subtracting the CN contribution, the differential cross sections at

Table 1
Experimental angular distribution of ^{11}C(d, n)^{12}N reaction at $E_{cm} = 9.8$ MeV

Annulation		θ_{cm} (°)	$\frac{d\sigma}{d\Omega}$ (mb/sr)
Forward angles	0	3.7 ± 6.5	53.4 ± 11.5
	1	16.0 ± 6.5	14.4 ± 3.1
	2	24.7 ± 7.0	5.1 ± 1.2
	3	33.8 ± 7.3	3.5 ± 0.7
	4	43.5 ± 8.2	2.0 ± 0.7
	5	54.8 ± 9.7	1.6 ± 0.5
Middle angles	$6+7+8+9$	95.1 ± 38.0	0.35 ± 0.12
Backward angles	$0+1$	172.3 ± 7.6	9.0 ± 15.1
	$2+3$	156.5 ± 9.2	4.6 ± 2.6
	$4+5$	139.4 ± 11.6	0.64 ± 0.50

four forward angles ($\theta_{cm} \leqslant 33.8°$) were adopted to extract the ANC for the direct capture reaction ^{11}C(p, γ)^{12}N through a DWBA analysis [17]. The DWBA angular distributions in Fig. 4 have been corrected for finite angular resolution discussed above. The DWBA analysis of nucleon transfer reactions was usually used to extract spectroscopic factors. However, the spectroscopic factors have significant uncertainties associated with the choice of optical potentials from which the single particle wave functions in initial and final nuclei are calculated. For the proton transfer reaction $d + {}^{11}C \to n + {}^{12}N$, which includes two virtual decays, $d \to p + n$ and $^{12}N \to p + {}^{11}C$, the differential cross sections with CN contribution subtracted can be expressed in the form [18],

$$\left(\frac{d\sigma}{d\Omega}\right)_{exp} - \left(\frac{d\sigma}{d\Omega}\right)_{CN} = \sum_{j_i j_f} \left(C^{d}_{l_i j_i}\right)^2 \left(C^{^{12}N}_{l_f j_f}\right)^2 \frac{d\sigma^{DW}_{l_f j_f l_i j_i}/d\Omega}{b^2_{l_i j_i} b^2_{l_f j_f}}, \tag{1}$$

where $(d\sigma/d\Omega)_{exp}$, $(d\sigma/d\Omega)_{CN}$ and $d\sigma^{DW}_{l_f j_f l_i j_i}/d\Omega$ refer to the measured, CN and reduced DWBA cross sections, respectively, and l_i, j_i and l_f, j_f stand for the orbital and total angular momenta of the transferred proton in initial and final nuclei d and ^{12}N, respectively, $b_{l_i j_i}$ and $b_{l_f j_f}$ are the single particle ANCs of the bound–state proton in d and ^{12}N, respectively. In the case of peripheral transfer reactions, the ratio in Eq. (1) is approximately of model independence as pointed out in Ref. [19], in turn, the ANCs are less model dependent and thus the best quantities for parameterizing the cross section. Given the ANC for the virtual decay $d \to p + n$, $C^{d}_{l_i j_i}$, the unknown ANC for the direct capture reaction ^{11}C(p, γ)^{12}N can be extracted from the DWBA analysis.

In the present DWBA analysis, the ratio of $p_{3/2} : p_{1/2}$ was taken as 0.18 from shell model calculations [6]. The ANCs for $^{12}N \to p + {}^{11}C$ were found to be $(C^{^{12}N}_{p_{1/2}})^2 = 2.43 \pm 0.77$ fm^{-1}, $(C^{^{12}N}_{p_{3/2}})^2 = 0.44 \pm 0.16$ fm^{-1} and the total ANC was $(C^{^{12}N}_{p_{eff}})^2 = (C^{^{12}N}_{p_{1/2}})^2 + (C^{^{12}N}_{p_{3/2}})^2 = 2.86 \pm 0.91$ fm^{-1}. The error was caused by statistics (18%), deviation from optical potentials in the entrance and exit channels used in DWBA calculation (6%), uncertainty of the ratio of $p_{3/2} : p_{1/2}$ (3%) and uncertainty from spectroscopic factor fitting (25%). The large uncertainty of spectroscopic factor fitting arose from the deviation between the measured angular distribution and DWBA calculated ones at forward angles.

Table 2
The optical potential parameters used in DWBA calculation and the corresponding spectroscopic factors, where V and W are in MeV, R and a in fm

Set No.	1		2		3		4		5	
Channel	in	out	in	out	in	out	in	out	in	out
V_r	108.7	49.9	110.4	49.9	110.4	50.9	110.4	46.5	110.4	62.8
R_r	1	1.2	1	1.2	1	1.2	1	1.4	1	1.14
a_r	0.8	0.65	0.8	0.65	0.8	0.65	0.8	0.4	0.8	0.57
W	5.01		4.43		4.43		4.43		4.43	
R_w	1		1		1		1		1	1.14
a_w	0.8		0.8		0.8		0.8		0.8	0.5
$4W_s$	20.04	18.96	17.72	18.96	17.72	17.48	17.72	26	17.72	26.7
R_s	2	1.2	2	1.2	2	1.2	2	1.05	2	1.14
a_s	0.6	0.47	0.6	0.47	0.6	0.47	0.6	0.4	0.6	0.5
$4V_{so}$	28.6	28	29.04	28	29.04	28	29.04	22	29.04	22
R_{so}	1	1.2	1	1.2	1	1.2	1	1.2	1	1.14
a_{so}	0.8	0.65	0.8	0.65	0.8	0.65	0.8	0.4	0.8	0.57
R_c	1.5		1.5		1.5		1.5		1.5	
$S_{j=1/2}$	1.19 ± 0.37		1.15 ± 0.37		1.14 ± 0.36		0.96 ± 0.30		1.09 ± 0.33	
$S_{j=3/2}$	0.21 ± 0.08		0.21 ± 0.08		0.21 ± 0.08		0.17 ± 0.06		0.20 ± 0.07	

This deviation may be caused by the difference between the optical potential parameters taken from the closest stable interacting systems [20] and those for the $d + {}^{11}C$ and $n + {}^{12}N$ systems which are not currently available. The optical potential parameters are listed in Table 2, together with the corresponding spectroscopic factors S_{lj} which relate to C_{lj} via the equation $C_{lj}^2 = S_{lj} b_{lj}^2$.

3. Theoretical analysis of ^{11}C(p, γ)^{12}N reaction

The ^{11}C(p, γ)^{12}N cross section for direct E1 radiative capture of proton to the ground state of ^{12}N was calculated by assuming that both the initial and final states of the system can be described by a single particle model of a proton moving in an optical potential that represents its interaction with the ^{11}C ground state. The amplitude of this process can be written as

$$T_{1m} = \left\langle I^{^{12}N}_{p\,^{11}C}(\vec{r}) \middle| e_{\text{eff}} r Y_{1m}(\Omega) \middle| \psi^{(+)}_{\vec{k}}(\vec{r}) \right\rangle, \tag{2}$$

where the effective charge $e_{\text{eff}} = eN/A$ for proton capture reaction, N and A are the neutron and mass numbers of the whole system, respectively. $\psi^{(+)}_{\vec{k}}(\vec{r})$ stands for the entrance channel distorted wave function, describing the relative motion between ^{11}C and proton in the continuum with the incident wave number vector $\vec{k}$. The overlap function of the bound state wave functions of ^{12}N, ^{11}C and proton is given by

$$I^{^{12}N}_{p\,^{11}C}(\vec{r}) = \left\langle \phi_P(\xi_P) \phi_{^{11}C}(\xi_{^{11}C}) \middle| \phi_{^{12}N}(\xi_P, \xi_{^{11}C}, \vec{r}) \right\rangle, \tag{3}$$

where $\vec{r}$ is the distance vector between the centers of mass of proton and ^{11}C, and ξ_s are the intrinsic coordinates for the particles labeled by their subscripts. The radial part of the

overlap function, $I_{\ell_f j_f}(r)$, defined in the multipole expansion of $I^{^{12}\mathrm{N}}_{\mathrm{p}^{11}\mathrm{C}}(\vec{r})$, depends on the relative orbit angular momentum ℓ_f of the captured proton and the ^{11}C core in the bound state j_f of ^{12}N. At very low energies of astrophysical interest, the capture reaction is almost totally peripheral and thus the radial overlap function has the asymptotic behavior

$$I_{\ell_f j_f}(r) = C_{\ell_f j_f} W_{\eta,\ell_f+1/2}(2\kappa r)/r, \quad r \geqslant R_N, \tag{4}$$

where $C_{\ell_f j_f}$ refers to the ANC, the amplitude of the tail of the radial overlap integral. R_N denotes the nuclear interaction radius between proton and ^{11}C, which is empirically taken as $\sim$4 fm in the present calculation. $W_{\eta,\ell_f+1/2}(2\kappa r)$ represents the Whittaker function, the wave number for the bound state $\kappa = \sqrt{2\mu E_B}/\hbar$ (μ and E_B being the reduced mass and the binding energy, respectively).

For s-wave scattering, the total cross section for E1 capture of proton to the ground state of ^{12}N with the orbit and total angular momenta ℓ_f and j_f can be expressed as

$$\sigma_{\mathrm{t}} = \frac{16\pi}{9}\left(\frac{E_\gamma}{\hbar c}\right)^3 \frac{1}{\hbar v}\frac{e^2_{\mathrm{eff}}}{k^2}\frac{(2j_f+1)}{(2I_1+1)(2I_2+1)} C^2_{\ell_f j_f} \times \left| \int_{R_N}^{\infty} r^2 \mathrm{d}r\, f_{\ell j}(kr) W_{\eta,\ell_f+1/2}(2\kappa r) \right|^2, \tag{5}$$

where E_γ, v, I_1 and I_2 are the γ-ray energy, relative velocity between particles 1 and 2, spin of ^{11}C and spin of ^{12}N, respectively. For the reaction discussed above, the distorted radial wave function in the entrance channel, $f_{\ell j}(kr)$, is the well-known Coulomb function, $k = \sqrt{2\mu E_{\mathrm{cm}}}/\hbar$ stands for the incident wave number. Consequently the cross section given by Eq. (5) and overall renormalization of the astrophysical S-factor for the reaction depend on the ANC only.

We have then calculated the S-factor as a function of E_{cm} for the direct capture reaction $^{11}\mathrm{C}(\mathrm{p},\gamma)^{12}\mathrm{N}$, as shown in Fig. 5. The direct capture S-factor at zero energy was found to be 0.157 ± 0.050 keV b through an extrapolation.

In this work the cross sections and the S-factors for 2^+ ($E_{\mathrm{cm}} = 0.360$ MeV) and 2^- ($E_{\mathrm{cm}} = 0.591$ MeV) resonances were calculated by the Breit–Wigner formula for a single-level resonance [21]. The proton and radiative widths for 2^+ resonance were taken as 5.5 keV [4] and 2.59 meV [1], respectively, and those for 2^- resonance 118 ± 14 keV [22] and 13 meV [5]. The resulting S-factors as a function of E_{cm} are shown in Fig. 5, as compared with that of the direct capture. The total S-factor includes the contributions of direct and resonant captures and that of the interference between direct capture and 2^- resonance which was considered in the way described in Ref. [23]. It can clearly be seen from Fig. 5 that the total S-factor is dominated by the direct capture in the wide energy range except the ranges corresponding to two resonances, and significantly enhanced by the interference in the energy range of $E_{\mathrm{cm}} < 0.6$ MeV.

We calculated the $^{11}\mathrm{C}(\mathrm{p},\gamma)^{12}\mathrm{N}$ reaction rates for stellar temperatures from $T_9 = 0.2$ to 0.6 using $\mathrm{S}(E_{\mathrm{cm}})$ given in Fig. 5. For the 2^- resonance with a large total width, the reaction rate was calculated by numerical integration of the product of the cross section and Maxwellian velocity distribution [24]. Fig. 6 shows the resulting reaction rates vs. temperatures for both the direct and resonant captures. It is seen that the direct capture

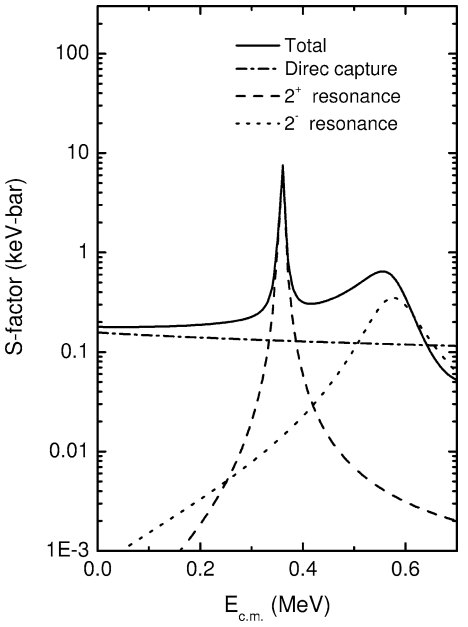

Fig. 5. E_{cm} dependence of the direct capture, resonant capture and total astrophysical S-factors for $^{11}\mathrm{C}(\mathrm{p},\gamma)^{12}\mathrm{N}$.

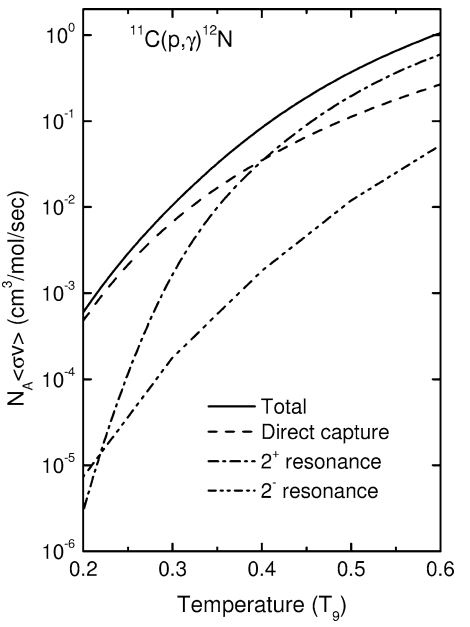

Fig. 6. Temperature dependence of the direct capture, resonant capture and total reaction rates for $^{11}\mathrm{C}(\mathrm{p},\gamma)^{12}\mathrm{N}$.

accounts for almost total of reaction rate at temperatures relevant to CNO chain ($T_9 = 0.02$) and novae ($T_9 = 0.3$).

It should be noticed that the theoretical value of $\Gamma_\gamma = 68$ meV [3] for the 2^- resonance state is larger than the experimental value used in our calculation by a factor of 5. We have performed the same calculation in which the theoretical value was used and all other parameters remained unchanged. The calculated result shows that the direct capture contribution is still larger than that of the 2^+ and 2^- resonances in a wide range of temperature.

4. Summary and conclusion

In this work, we have measured the angular distribution of the $^{11}\mathrm{C}(\mathrm{d},\mathrm{n})^{12}\mathrm{N}$ reaction and indirectly determined the direct capture S-factor and the rate for the $^{11}\mathrm{C}(\mathrm{p},\gamma)^{12}\mathrm{N}$ reaction at astrophysical energies, using the ANC for virtual decay $^{12}\mathrm{N} \rightarrow {}^{11}\mathrm{C} + \mathrm{p}$. In addition, we have also calculated the contributions of the resonant captures into the first and second excited states of $^{12}\mathrm{N}$ and the interference between direct capture into the ground state and resonant capture into the second excited state. In contrast to the prediction in Ref. [3], our results show that the direct capture dominates the $^{11}\mathrm{C}(\mathrm{p},\gamma)^{12}\mathrm{N}$ in the wide energy range of astrophysical interest except the ranges corresponding to two resonances. The similar conclusions were also demonstrated in Refs. [7] and [6] though their direct capture S-factors are smaller than ours by factors of about 0.6 and 0.7–0.9, respectively.

The direct measurement for the $^{11}C(p,\gamma)^{12}N$ reaction which is conducive to clarify some discrepancies for both the direct and resonant captures might be realizable in the near future with the development of secondary beam facility.

Acknowledgements

The authors wish to thank Prof. Zhongdao Lu and Prof. Yinlu Han for their help in Monte Carlo simulation and CN calculation, respectively. This work was supported by the Major State Basic Research Development Program under Grant No. G200077400 and the National Natural Science Foundation of China under Grant Nos. 19735010, 19935030, 10025524, 10045002 and 10075078.

References

[1] M. Wiescher, J. Görres, S. Graff, L. Buchmann, F.-K. Thielemann, Astrophys. J. 343 (1989) 352.
[2] P. Descouvemont, I. Baraffe, Nucl. Phys. A 514 (1990) 66.
[3] P. Descouvemont, Nucl. Phys. A 646 (1999) 261.
[4] A. Lefebvre, P. Aguer, J. Kiener, G. Bogacrt, A. Coc, F. de Oliveira, J.P. Thibaud, D. Disdier, L. Kraus, I. Linck, S. Fortier, J.A. Scarpaci, C. Stephan, L. Tassan-Got, Ph. Eudes, F. Guilbault, Th. Reposeur, C. Grunberg, P. Roussel-Chomaz, F. Attallah, Nucl. Phys. A 592 (1995) 69.
[5] T. Minemura, et al., RIKEN Accel. Prog. Rep. A 35 (2002).
[6] N.K. Timofeyuk, S.B. Igamov, Nucl. Phys. A 713 (2003) 217.
[7] X. Tang, A. Azhari, C.A. Gagliardi, A.M. Mukhamedzhanov, F. Pirlepesov, L. Trache, R.E. Tribble, V. Burjan, V. Kroha, F. Carstoiu, Phys. Rev. C 67 (2003) 015804.
[8] H.M. Xu, C.A. Gagliardi, R.E. Tribble, Phys. Rev. Lett. 73 (1994) 2027.
[9] W. Liu, X. Bai, S. Zhou, Z. Ma, Z. Li, Y. Wang, A. Li, Z. Ma, B. Chen, X. Tang, Y. Han, Q. Shen, Phys. Rev. Lett. 77 (1996) 611.
[10] A. Azhari, V. Burjan, F. Carstoiu, H. Dejbakhsh, C.A. Gagliardi, V. Kroha, A.M. Mukhamedzhanov, L. Trache, R.E. Tribble, Phys. Rev. Lett. 82 (1999) 3960.
[11] A. Azhari, V. Burjan, F. Carstoiu, C.A. Gagliardi, V. Kroha, A.M. Mukhamedzhanov, X. Tang, L. Trache, R.E. Tribble, Phys. Rev. C 60 (1999) 055803.
[12] N. Imai, N. Aoi, S. Kubono, D. Beaumel, K. Abe, S. Kato, T. Kubo, K. Kumagai, M. Kurokawa, X. Liu, A. Mengoni, S. Michimasa, H. Ohnuma, H. Sakurai, P. Strasser, T. Teranishi, M. Ishihara, Nucl. Phys. A 688 (2001) 281c.
[13] X. Bai, W. Liu, J. Qin, Z. Li, S. Zhou, A. Li, Y. Wang, Y. Cheng, W. Zhao, Nucl. Phys. A 588 (1995) 273c.
[14] W. Liu, Z. Li, X. Bai, Y. Wang, G. Lian, S. Zeng, S. Yan, B. Wang, Z. Zhao, T. Zhang, H. Tang, B. Yang, X. Guan, B. Cui, Nucl. Instrum. Methods Phys. Res. B 204 (2003) 62.
[15] Z. Li, W. Liu, X. Bai, Y. Wang, G. Lian, Z. Li, S. Zeng, Phys. Lett. B 527 (2002) 50.
[16] J. Zhang, UNF Code for fast neutron reaction data calculations, Nucl. Sci. Eng. 142 (2002) 207.
[17] P.D. Kunz, Computer code DWUCK4.
[18] A.M. Mukhamedzhanov, H.L. Clark, C.A. Gagliardi, Y.-W. Lui, L. Trache, R.E. Tribble, H.M. Xu, X.G. Zhou, V. Burjan, J. Cejpek, V. Kroha, F. Carstoiu, Phys. Rev. C 56 (1997) 1302.
[19] A.M. Mukhamedzhanov, C.A. Gagliardi, R.E. Tribble, Phys. Rev. C 63 (2001) 024612.
[20] C.M. Perey, F.G. Perey, At. Data Nucl. Data Tables 17 (1976) 45.
[21] J.M. Blatt, V.F. Weisskopf, Theoretical Nuclear Physics, Wiley, New York, 1952.
[22] F. Ajzenberg-Sclove, Nucl. Phys. A 637 (1998) 576.
[23] L. Buchmann, J.M. D'Auria, P. McCorquodale, Astrophys. J. 324 (1988) 953.
[24] C.E. Rolfs, W.S. Rodney, Cauldrons in the Cosmos, University of Chicago Press, Chicago, 1988.